

Cell Reports, Volume 25

Supplemental Information

Recording Neural Activity in Unrestrained Animals

with Three-Dimensional Tracking

Two-Photon Microscopy

Doycho Karagyzov, Mirna Mihovilovic Skanata, Amanda Lesar, and Marc Gershow

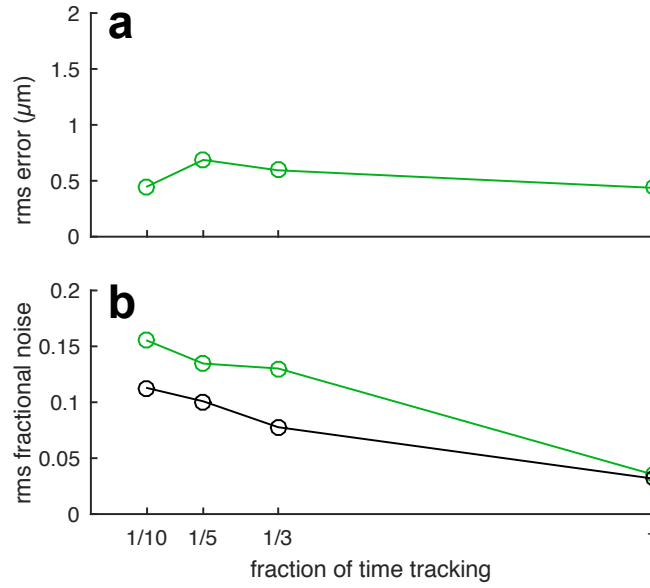


Figure S1: Tracking error and fluorescence noise vs. tracking duty cycle. Related to Figure 1. For a 10 Hz $20\ \mu\text{m}$ peak-to-peak in-plane sinusoidal oscillation, the root-mean-squared (rms) positional error (a) and rms noise in fluorescence (b), if only indicated fraction of cycles are used for measurement and tracking.

Fig 2a, before tracking

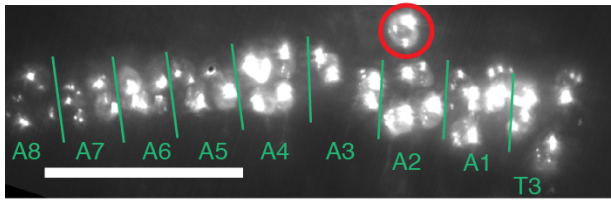


Fig 3, before bleaching off-target neurons and tracking

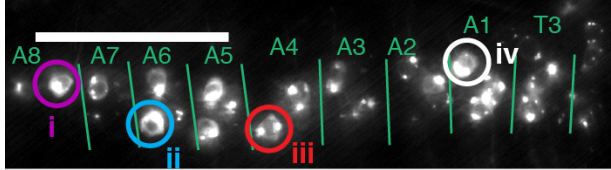


Fig 4, before bleaching off-target neurons and tracking

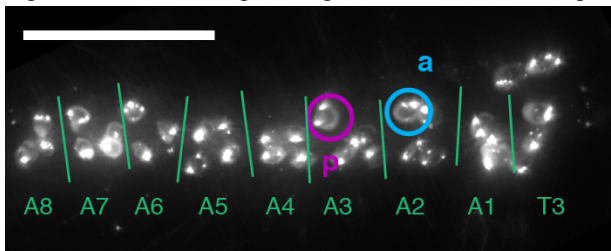
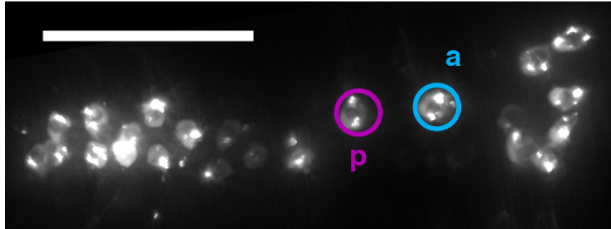


Fig 4, after bleaching off-target neurons and tracking



posterior

anterior

Figure 5 - schematic of neuron locations

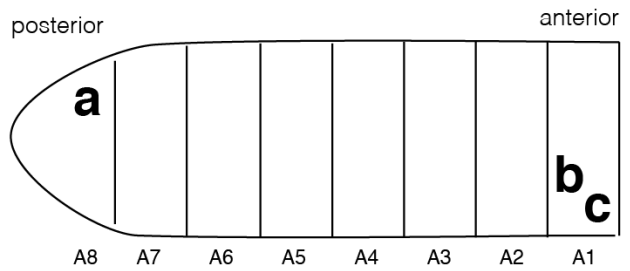


Fig 5a, before bleaching off-target neurons and tracking

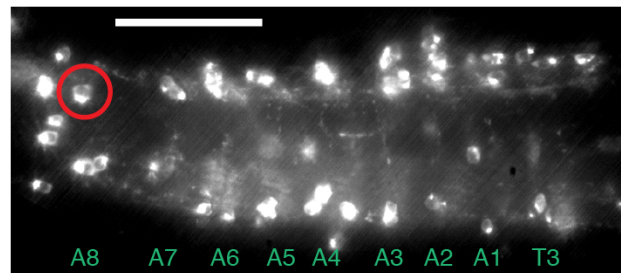


Fig 5b, before bleaching off-target neurons and tracking

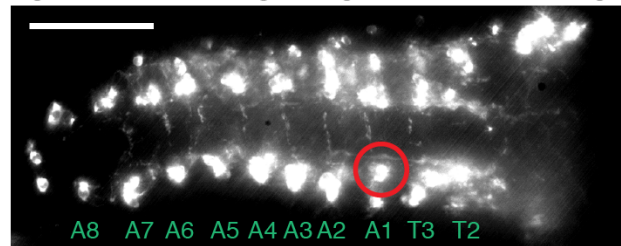
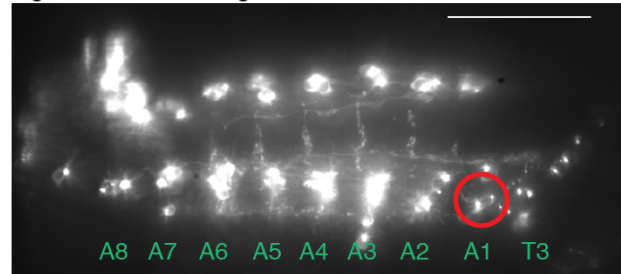


Fig 5c, before tracking



posterior

anterior

Figure S2: Epifluorescence images of tracked VNC neurons. Related to **Figure 2, Figure 3, Figure 4, and Figure 5** Epifluorescence images of mCherry labeling of neurons. Neurons whose activities are shown in the corresponding figures are indicated by colored circles. Displayed images are a maximum intensity projection of images taken at several depths, with brightness and contrast adjusted in ImageJ. Clustering of mCherry can be seen in these images; this clustering did not affect our ability to track neurons. These images were all taken while the larva was immobilized by compression, which could distort brain geometry relative to the uncompressed state. Fig 2a,3,4,5 – annotations mark our estimate for segment locations, based on cell body positions. A schematic of the cell body locations for **Figure 6a-c** is shown above the Fig 6 epifluorescence images. Fig 5: RG3602 also labels a second set of VNC neurons in a different plane from the neurons shown and tracked here. All images: scale bar is 50 μ m.

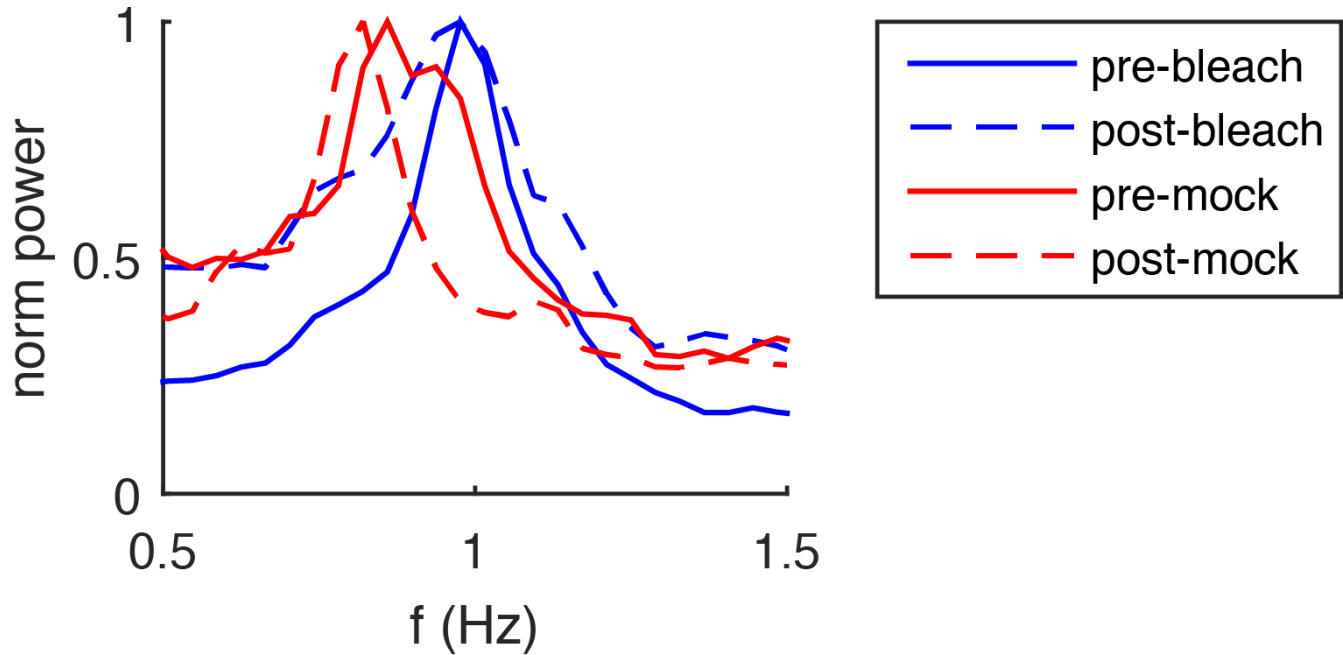


Figure S3: Power spectra of peristaltic motion before and after photobleaching motor neurons Related to **Figure 3** Larvae expressing *GCaMP6f* and hexameric *mCherry* in motor neurons were recorded crawling on an agar gel under infrared illumination. The tail location was determined at a frame rate of 20Hz and the power spectrum of the instantaneous tail velocity is shown in the range 0.5-1.5 Hz and normalized so that the peak power in this range is 1. Pre-bleach: initial recording of the larvae. Post-bleach: the same larvae were immobilized in the microfluidic device, VNC neurons were located in epifluorescence and then bleached under high two photon excitation power. Following a period of recovery from the compression, larvae were re-imaged crawling on an agar gel. $n = 8$ larvae. Pre/post-mock: on a different day, the same protocol was applied, except the excitation power was kept at the level usually used for imaging. $n = 3$ larvae

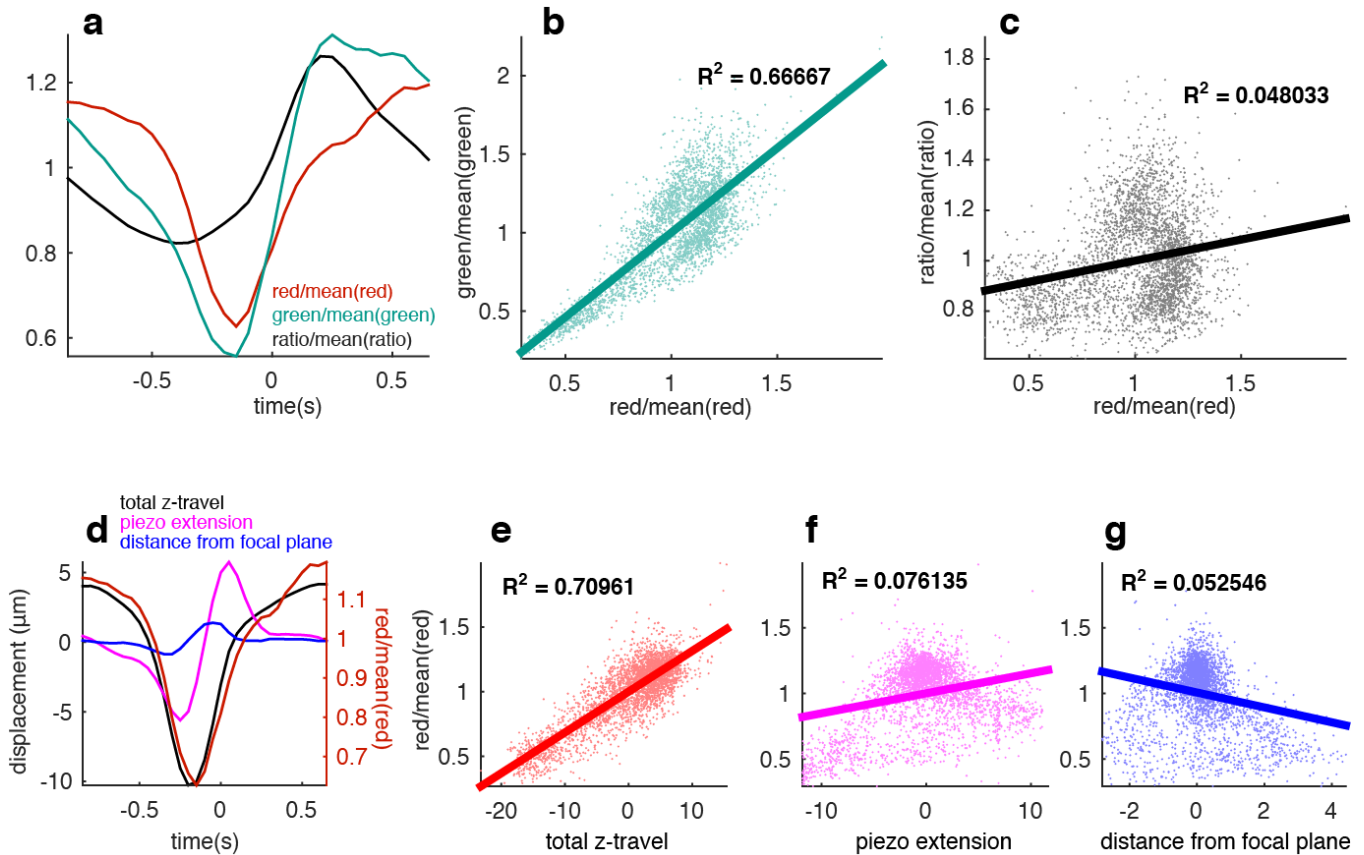


Figure S4: Fluctuations in recovered fluorescence in an uncompressed larva Related to **Figure 5 (a)** Cycle averaged red count rate, green count rate, and ratio of green to red, for the neuron and data shown in **Figure 5c**. Each trace is normalized by the mean value per cycle. **b,c** Scatter plots showing instantaneous normalized green count rate (**b**) and red/green ratio (**c**) vs. normalized red count rate and linear fits. **d** Left axis: Cycle averaged displacement of the neuron from its average position during the cycle as well as cycle averaged extension of the piezo objective and cycle averaged distance of the neuron from the natural focal plane of the objective. Right axis: cycle averaged normalized red count rate. **e-g** Scatter plots and linear fits showing instantaneous normalized red count rate vs. total displacement of the neuron, extension of the piezo, and distance of the neuron from the natural focal plane.

The red fluorescence is due to the calcium insensitive protein mCherry. The green fluorescence is due to the calcium sensitive protein GCaMP6f. The green photon count rate varies due to both motion and neuronal calcium concentration, while the red count rate varies due to motion only. The ratiometric measure of activity, which is designed to vary only with neuronal calcium concentration, obeys different temporal dynamics and is not obviously correlated with the motion-associated fluctuation in the red count rate (**a-c**). If the changes in the ratiometric activity measure were due to motion artifacts, they would necessarily be correlated with and in temporal phase with the changes in recovered red fluorescence.

The changes in red fluorescence almost exactly track the vertical displacement of the neuron over the course of the cycle (**d,e**). The z-motion of the neuron is compensated first by changing the phase of acquisition relative to the TAG lens cycle, then by motion of the piezo objective and finally by motion of the stage. That the motion-associated changes in the red fluorescence are most strongly correlated with the actual movement of the neuron and not with the extension of the piezo (**f**) or the TAG-compensated displacement of the neuron relative from the natural focal of the objective suggests that these changes are due to physical changes in the larva. IE if the the collection efficiency varied strongly as the neuron moved from the natural focal plane, this would be reflected a strong correlation between the red signal and focal plane displacement. One candidate physical change would be that muscle-induced contraction of the segment of cuticle between the tracked neuron and the microscope objective increases scattering in the light path. If, as we argue, the change in recovered fluorescence efficiency is due to properties of the larva and not to the specifics of our microscope, this implies that ratiometric correction is required for optical recording in VNC and central brain neurons in many common geometries.

Fig 6a, before tracking

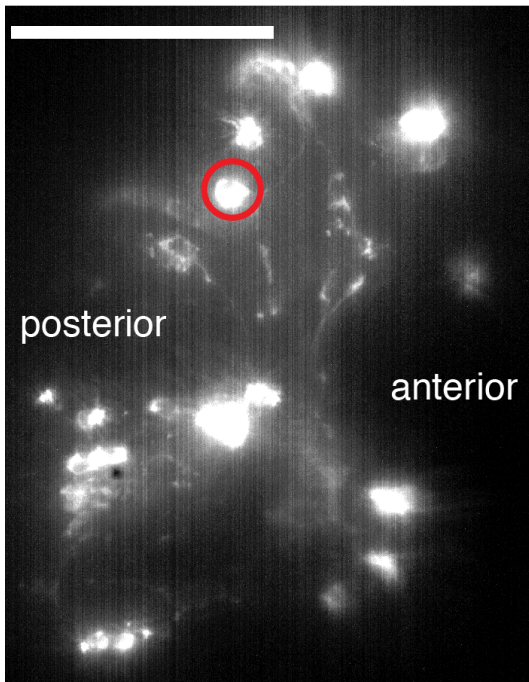


Fig 6g, before bleaching off-target neurons and tracking

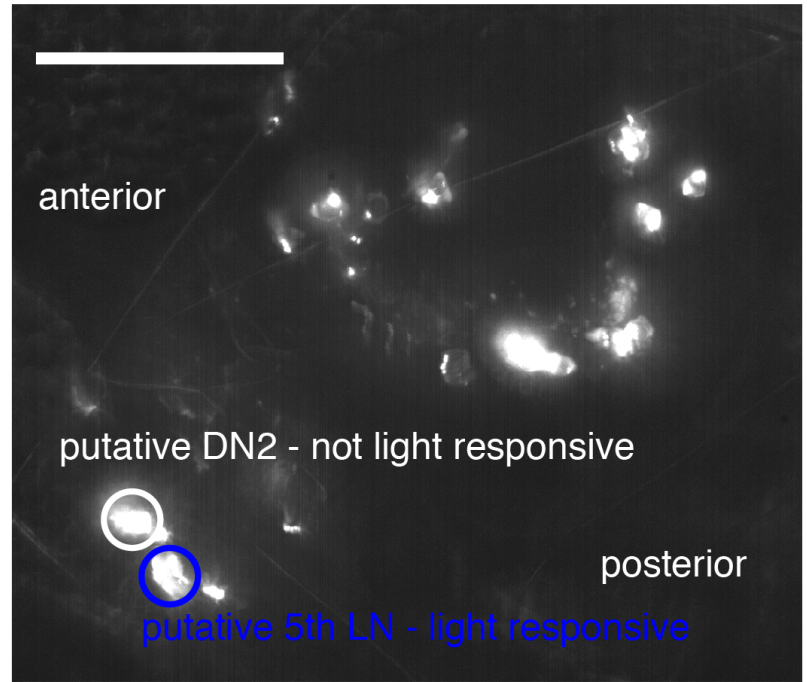


Fig 6h, before tracking

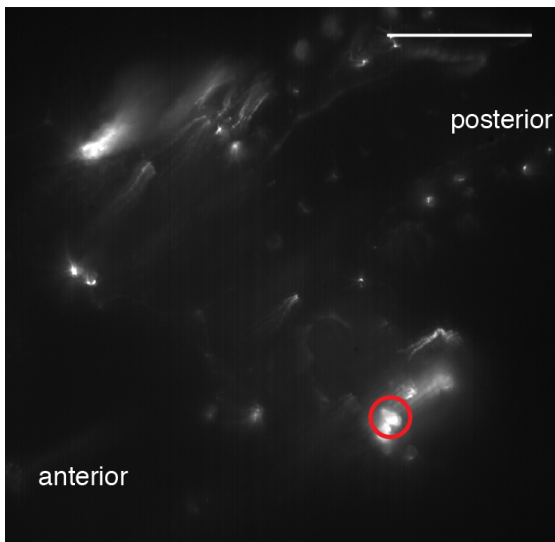


Fig 6h, 10 individual traces

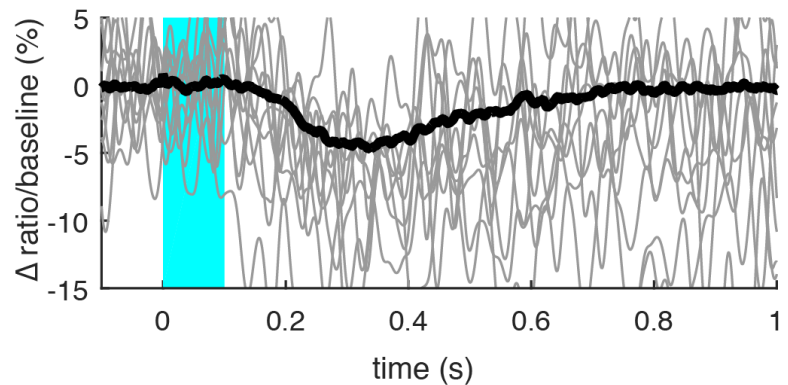


Figure S5: Epifluorescence images of tracked visual interneurons and individual traces for voltage recording. Relates to **Figure 6** Epifluorescence images of mCherry labeling of neurons. Neurons whose activities are shown in the corresponding figures are indicated by colored circles. Displayed images are a maximum intensity projection of images taken at several depths, with brightness and contrast adjusted in ImageJ. Clustering of mCherry can be seen in these images; this clustering did not affect our ability to track neurons. These images were all taken while the larva was immobilized by compression, which could distort brain geometry relative to the uncompressed state. All images: scale bar is 50 μm . Individual traces: Change in ratio of green/red indicator for 10 randomly selected traces (light line) and mean of 400 traces (dark line) from voltage imaging experiment shown in **Figure 6h**. ASAP2s decreases in brightness with increasing internal voltage. Recordings are aligned to the onset of blue light stimulus and shaded region indicates time when stimulus was on.